Available online at www.sciencedirect.com
ScienceDirect
Ceramics International 33 (2007) 1179–1185
CERAMICS INTERNATIONAL
www.elsevier.com/locate/ceramint

Activation of alumina foams for fabricating MMCs by pressureless infiltration

K. Lemster, M. Delporte, T. Graule, J. Kuebler *

Empa, Materials Science and Technology, Laboratory for High Performance Ceramics, Ueberlandstr. 129, 8600 Duebendorf, Switzerland

Received 26 January 2006; received in revised form 2 March 2006; accepted 9 April 2006
Available online 11 September 2006

Abstract

Metal matrix composites (MMC) combine the properties of metals and ceramics to yield failure tolerant materials. Using ceramic foams, these composites become three-dimensional structures of intimately connected metal and ceramic which should possess, e.g. high wear resistance. Once the problem of inherently poor wetting of ceramic by metal melts is eliminated, MMCs can be produced by spontaneous infiltration of metal into a ceramic structure, i.e. by pressureless infiltration. At the crucial infiltration step, an activator such as elemental titanium must be spread over the ceramic surface. In contact with the melt, the elemental Ti significantly improves the wetting, so that the metal can spontaneously infiltrate the ceramic structure. In this study, a halide salt route and a wet TiH_2 route were investigated as activation methods with which to generate Ti activation in alumina foams. Both methods enabled activation of alumina foams within the range of 20–90 pores per inch (ppi) pore size and promoted spontaneous metal infiltration of Inconel 625 and X38CrMoV5-1 into the activated structures.

Keywords: B. Composite; D. Al_2O_3; E. Wear parts; MMC pressureless infiltration

1. Introduction

Metal matrix composites (MMCs) have been developed in order to combine the advantageous properties of both ceramics and metals into a single material. Amongst the many types of MMCs, some are reinforced with porous ceramics and ceramic foams. These exhibit fine and continuous three-dimensional interconnected ceramic/metal networks, which provide the MMC with a high structural homogeneity and good ceramic to metal bonding. Each phase contributes to the properties of the final composite, with the metal part increasing the strength and the fracture toughness relative to the monolithic ceramic, and the ceramic part increasing the dimensional and mechanical stability at high temperatures relative to the pure metal [1–3]. MMCs are also failure tolerant, meaning that localized failures in the material do not immediately lead to spontaneous failure of the entire component.

Potential applications for MMC components are a large variety of wear parts in a range of market sectors including electronic waste recycling, mining and metal forming [4]. For example, MMCs are of great interest for matrices and punches for the cold working of thin and thick-walled metal sheets, for local reinforcement at the edges of cutting tools, and for running surfaces in friction bearings.

However, due to the poor wettability of ceramics by metal melts, the fabrication of MMCs can generally only be achieved by forced infiltration of the metal in the ceramic structure. External pressure to achieve infiltration can be applied, for example, by squeeze casting [5,6] or with gas pressure [1,2,7]. By applying an external pressure, it is possible to overcome the wetting difficulty, however, a relatively high level of technological complexity is needed and the methods possess some intrinsic limitations. Due to economic reasons, squeeze casting is not feasible for MMCs with Fe, Fe-base alloys, Ni or Ni-base with melting points well above 1000 °C. Thus, this latter technique in practice is mostly used for low melting point metals and alloys (e.g. Al, Al alloys, Mg, Ag or bronze) which have melting points well below 1000 °C.

An interesting alternative for the preparation of MMCs is the pressureless infiltration method. In this approach, so-called activation of the ceramic is required to overcome the metal melt/ceramic wetting problem. Activating the ceramic is thus a

* Corresponding author. Tel.: +41 44 823 4223; fax: +41 44 823 4150.
E-mail address: jakob.kuebler@empa.ch (J. Kuebler).

0272-8842/$32.00
doi:10.1016/j.ceramint.2006.04.002

crucial processing step. For decades, active elements such as Ti and Cr have been added to brazing solders for joining ceramic components. In these cases, the surface tension of the metal melt – and thereby the wetting angle θ at the interface ceramic metal – is decreased by formation of a reaction layer [8]. The addition of Ti to many non-reactive metal melts, for example, Cu [9] and Ni [10], results in a transition from non-wetting to wetting behavior on Al_2O_3 substrates. Lemster et al. [11] have shown that the process of Ti-activated melt infiltration is suitable for the combination of Al_2O_3 with Fe-base alloys as well as with Ni-base alloys, although in these cases no reaction layer could be detected at the ceramic/metal interface of the final MMC.

Pressureless activated infiltration is not limited to high melting alloys, and it has been used for a variety of metal/ceramic combinations like SiC/bronze, AlN/cast iron [12], Al_2O_3 and different Fe-base and Ni-base alloys. This list is not exhaustive, and certainly new metal/ceramic combinations not considered to date might prove valuable in future. As existing metal alloys for special applications can be chosen and combined with a suitable ceramic component, MMCs fabricated using activated pressureless infiltration have great potential as wear resistant materials for many other applications besides metal forming tools [13], e.g. as ball bearings.

Ti-activation has to date generally been achieved by introducing elemental Ti particles into the particle system being considered. In the case of the fine three-dimensional ceramic network mentioned above, a different activation route is required because such Ti particles can only penetrate large pore structures. In the current work, alumina foams were activated by introducing either inorganic or organic Ti-bearing compounds into ceramic preforms and subsequently heat-treating the preforms under a defined atmosphere to form elemental Ti. Three grades of foam with between 20 and 90 pores per inch (ppi) and two different activation routes were investigated. The first activation route involved a eutectic salt melt consisting of $CaCl_2$, KCl, NaCl and elemental Ti [14,15]. The second activation route used a suspension of TiH_2 and nitrocellulose binder. In both cases, the goal was to activate the ceramic network by forming localized spots of Ti over the ceramic in order to improve wetting and to achieve infiltration by high melting point alloys like Inconel 625 and X38CrMoV5-1.

2. Experimental

2.1. Preparation of foams

Ceramic foams with pore sizes from 20 to 90 ppi were prepared by the replica method [16,17].

2.1.1. Twenty to 80 ppi ceramic foams

For the halide salt route, the ceramic foams were produced by using polyurethane foams (PU) with 20, 30 or 80 ppi pore size (pore diameters of 1270, 850 and 320 μm, respectively). The water-based slurry consisted of 75 wt% alumina (Alcoa CT 3000 SG) with a carboxylic acid-based organic dispersant. After replication, the polymer was burned out (heating rate 40 °C/h up to 500 °C, 80 °C/h up to 1000 °C) and subsequently the ceramic structure was sintered (heating rate 300 °C/h up to 1000 °C, 60 °C/h up to 1550 °C with 1h holding time). The resulting 20 and 30 ppi ceramic foams were blocks of Ø 40 and 18 mm height, while the 80 ppi foams were blocks of Ø 35 and 27 mm height. This slurry composition worked well for the preparation of 20 and 30 ppi foam blocks, but the 80 ppi foam blocks were generally flawed with closed pores at the outer margins of the block and small cavities inside after sintering.

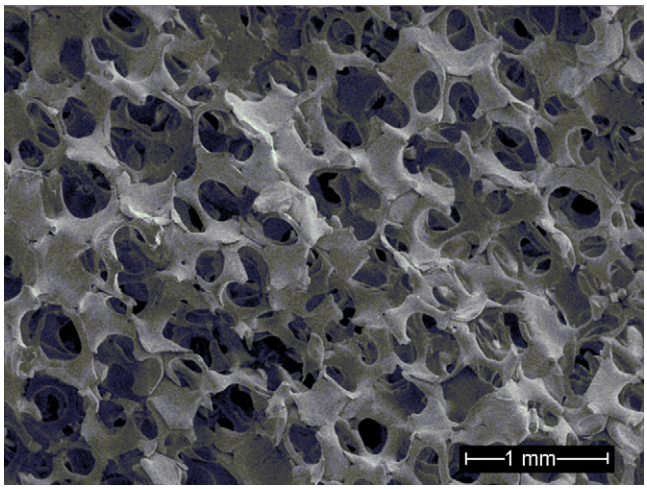

Fig. 1. Cross-section of a 90 ppi alumina foam prepared for TiH_2 activation.

2.1.2. Ninety ppi ceramic foams

These ceramic foams were also prepared starting with PU foams with a pore size of 90 ppi (average pore size of 280 μm). The slurry was a dispersion prepared by planetary milling of 70 wt% of alumina (Alcoa CT 3000 SG) in a water-based system with phosphoric acid as a dispersant. After replication and drying, the polymer foam was burned out and the ceramic part sintered at 1550 °C (heating rate 60 °C/h up to 1550 °C with 2 h holding time).

Fig. 1 shows an example of a 90 ppi alumina foam used in this work (Ø 40 mm × 12 mm high). While the initial PU foam porosity was 96 vol.%, the resulting total porosity after the replication process is 87 vol.%. The final foams have an average pore size of about 200 μm and struts approx. 50 μm in diameter.

2.2. Activation of ceramic foams

2.2.1. Activation via halide salt route

According to Lavendel [14] and Breval et al. [15], it is possible to obtain a continuous Ti coating on a non-metallic surface by way of a molten eutectic salt melt of NaCl, KCl and $CaCl_2$ mixed with Ti particles. During heat treatment (700–800 °C for 1 h, in argon atmosphere), Ti either dissolves or reacts with the molten halide salts and is chemisorbed on the alumina surface due to its affinity to oxygen.

Different proportions of the salts were used in this work compared to those used by Lavendel and Breval. The mixture

consisted of 36.8 wt% KCl, 29.9 wt% NaCl, 27.5 wt% $CaCl_2$ and 5.8 wt% Ti (325 mesh, $\leq$45 μm). This composition is shifted away from the eutectic composition, and consequently the melting point of this salt mixture is increased to ~550 °C. According to Breval, the salt mixtures must be soaked at temperatures between 200 and 300 °C above the melting point.

The salt mixture was first ground and intimately mixed with the Ti powder. The resulting powdered blend was introduced into the 20–80 ppi ceramic foams simply by vibrating it into the pores. The amount of salt mixture used was chosen so that the entire ceramic surface of given foam was completely covered.

The thermal treatment was carried out under argon at 750 °C with a holding time of 1 h (heating and cooling rate 8 °C/min). Residual salt was removed by rinsing the ceramic foams with water for about 8 h. The rinsing water was frequently renewed and periodically the samples were placed in an ultrasonic bath. Removal of the excess salt by washing revealed the underlying coating of titanium, which imparted the foams with a metallic grey coloration (Fig. 2).

2.2.2. Activation via TiH_2 route

The TiH_2 powder obtained from Alfa Aesar had an average particle size of 4.0 μm (d_{10} = 1.7 μm, d_{90} = 8.1 μm). The activation mixture was prepared by manual stirring of the TiH_2 powder with octylacetate as a solvent (Sigma–Aldrich) and dinitrate cellulose as a binder in the proportions 40/30/30 by weight, respectively. The cellulose binder was favored because of its low thermal stability, with thermal degradation of the cellulose skeleton being nearly complete at 400 °C [18]. Primarily volatiles are produced during the thermal degradation process and only little carbon residue remains, therefore, few TiC compounds are likely to be formed during the subsequent activation step.

Three ways were considered to introduce the TiH_2 mixture in the ceramic foam. By simply pouring the mixture on top of the foam, the preform was never completely activated because the capillary forces were not strong enough to draw the activation mixture through the foam to the opposite open face. By immersing the ceramic foams in the activator slurry this problem was overcome, however, the time required for the mixture to reach the center of the ceramic structure was deemed unacceptably long. The final and most efficient method was to pour the blend onto the top of the ceramic foam and then draw it through the pore structure by applying a vacuum under the foam. This method yielded a homogeneous distribution of TiH_2 all over the ceramic foams.

Prior to steel infiltration, the TiH_2 had to be reduced to metallic Ti. For this process the samples were placed in a reduction chamber (Fig. 3) consisting of two coaxial cylinders made of molybdenum. The gap in between the cylinders was filled up with Ti chips. While heating the reduction chamber up to 950 °C (5 °C/min up to 400 °C with 30 min holding time, 10 °C/min up to 950 °C with 30 min holding time) under vacuum (~10^{-5} mbar), the nitrocellulose-based binder first burned out at ~230 °C and dehydrogenation of TiH_2 started at 550–600 °C. The resulting organic products and hydrogen gases were pulled out by the vacuum while the Ti chips acted as oxygen getters to ensure a low oxygen content inside the reduction chamber.

2.3. Metal infiltration

For infiltration a conventional high vacuum furnace was used (Super VII, Centorr Vacuum Industries). A detailed description of processing of activated infiltration is published elsewhere [11].

The activated ceramic foam was placed inside a crucible and surrounded as well as covered with cleaned pieces of the respective alloy. In the case of the halide salt route, the activated ceramic foams were infiltrated with Inconel 625 (Ni > 58, Cr 20–23, Mo 8–10, Nb 3.15–4.15, Fe 5; melting point 1350 °C, W.Nr 2.4856 UNS N06625) under high vacuum (7×10^{-5} mbar) at 1600 °C (5 °C/min up to 1000 °C and 10 °C/min up to 1600 °C with 30 min holding time, cooling rate 10 °C/min).

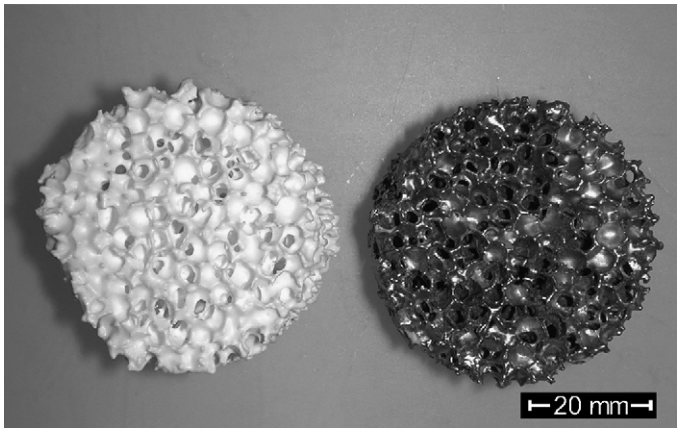

Fig. 2. A 30 ppi alumina foam before and after activation. The visible surfaces of the activated ceramic foam on the right are practically all colored grey by the metallic Ti.

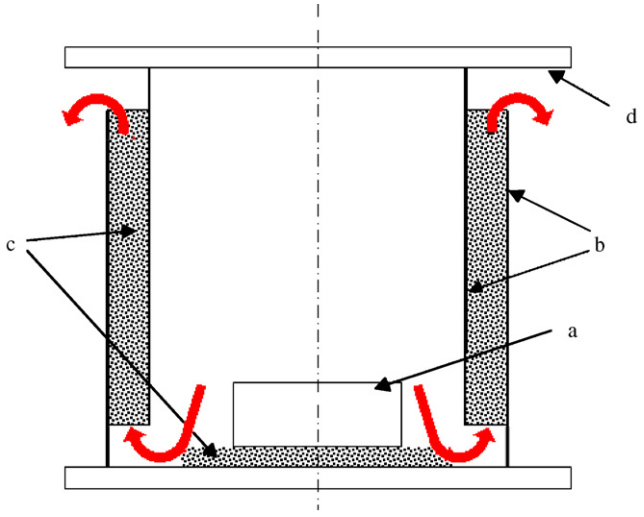

Fig. 3. Schematic cross-section through the reduction chamber. (a) Alumina foam filled with TiH_2, (b) coaxial cylinders of molybdenum, (c) Ti chips and (d) dense alumina cover.

For the TiH_2 route, the activated ceramic foams were infiltrated with steel (X38CrMoV5-1; melting point 1490 °C; W.Nr 1.2343) under high vacuum (7×10^{-5} mbar) at 1600 °C (5 °C/min up to 1000 °C with 30 min holding time, 10 °C/min up to 1600 °C with 30 min holding time).

2.4. Characterization

Characterization of the non-activated ceramic foams and the final MMC microstructures were carried out by optical microscopy (Zeiss Axiovert 100A with digital camera) and scanning electron microscopy (SEM; TESCAN Vega TS 5136MM; JEOL JSM-6300 with an energy dispersive spectroscope). Prior to the SEM investigations, the samples were embedded in a colored epoxy resin and polished. After activation, the crystallographic nature of the activator was qualitatively characterized using powder X-ray diffraction (XRD). For this analysis, the activated foams were ground to a fine powder and mounted on Si sample holders. Selected areas of the infiltrated MMCs were investigated by quantitative electron X-ray microprobe analysis (EPMA; JEOL JXA-8800RL).

3. Results and discussions

3.1. Halide salt route

Using the halide salt route, alumina foams of 20 and 30 ppi pore size were successfully coated with a metallic grey layer of Ti particles. This layer was obtained after extensive washing in order to get rid of the excess residual salts. Supported by ultrasonic treatment together with frequent water changes, the cleaning time could be reduced to 8 h. The thickness of the Ti particle layer finally obtained was estimated to be about 10 μm (Fig. 4).

In the case of the 80 ppi ceramic foams, only the first outer millimeters of the foam blocks could be activated. As mentioned earlier, these replicated foams featured closed pores, and furthermore the halide salts were relatively coarse compared to the pore size of the ceramic foam (320 μm). Therefore, it was difficult for the halide salt powder to penetrate the foam structure.

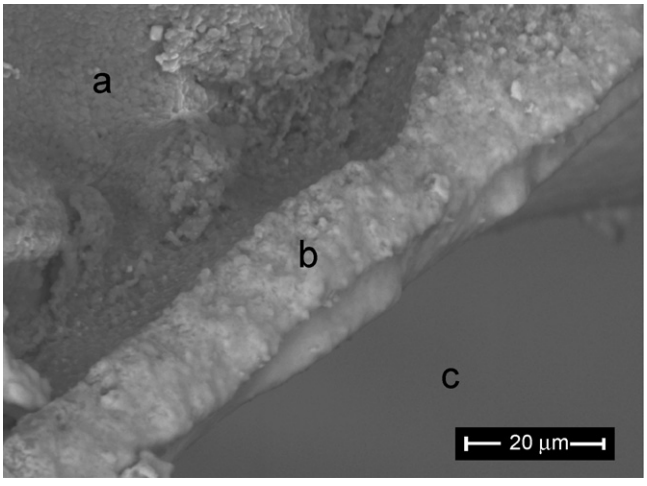

Fig. 4. SEM micrograph of the Ti particle layer of approximately 10 μm thickness on a 30 ppi alumina foam. (a) Alumina strut, (b) Ti layer and (c) hollow core of the strut.

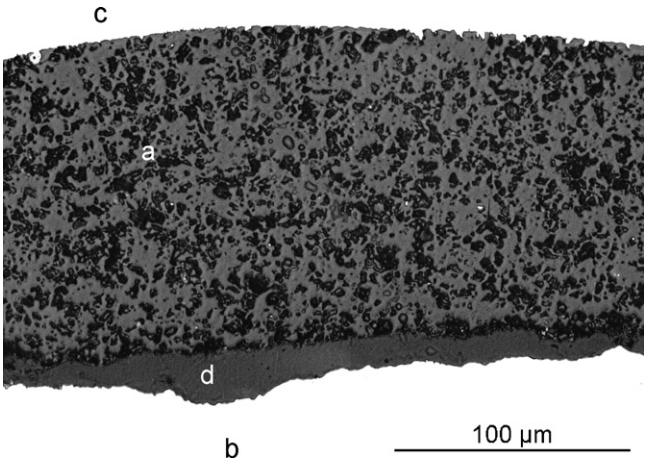

Fig. 5. Halide salt activated alumina foam after infiltration with Inconel 625. (a) Alumina strut, (b) main channel, i.e. pore, (c) hollow core of the strut and (d) gap between ceramic and metal filled embedding epoxy used for sample preparation.

The presence of Ti particles on the ceramic foam surfaces enabled infiltration of the structure by the molten Inconel alloy. The first experiments revealed the need for containments around the ceramic blocks during infiltration, so that the molten alloy could not flow out of the pores on the side of the block. Despite the successful infiltration of the activated foams, the bonding between metal and ceramic was sometimes inexistent (Fig. 5). At the interface between the ceramic strut and the metal, a gap of up to 10 μm could be observed in some cases. The cause for this could be a lack of melt during the infiltration which prevented complete filling of the main pore channels. Alternatively, the shrinkage of the metal melt during cooling and solidification might have caused considerable shrinkage in large pores which consequently created gaps between the ceramic and the metal. The cores of the struts which were hollow after burnout of the PU foam were also filled up by the melt and there, the ceramic and the metal were always continuously connected.

3.2. TiH_2 route

Activation by the TiH_2 route was successful. The foams were covered throughout by a metallic grey layer, however, the concentration of Ti particles was much higher on the side of the sample where the activator blend had been poured. Like a filter, the structure of the foams probably separated the powder from the fluid transport medium, resulting in accumulation of TiH_2 in the first few millimeters. This hypothesis was corroborated by BET surface area (Coulter SA3100) and particle size measurements (Malvern Mastersizer and Coulter LS230) which precluded any agglomeration effects due to either the powder or the binder.

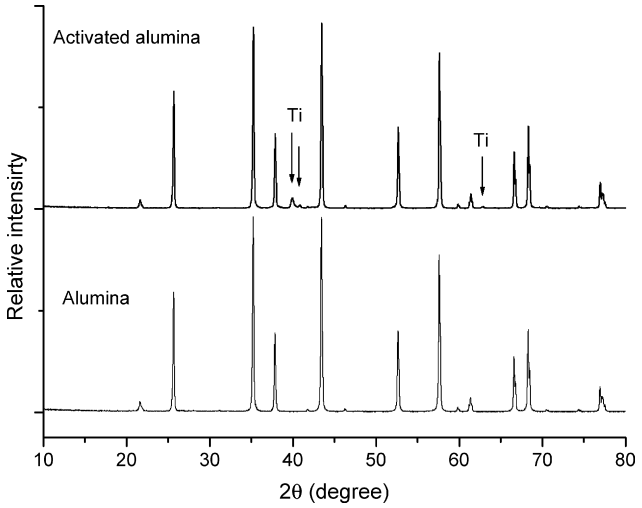

Fig. 6. XRD patterns of a non-activated alumina foam and an alumina foam activated via the TiH_2 route.

The kinetics of the dehydrogenation of TiH_2 to elemental Ti is a subject of ongoing research. Recently, Bhosle et al. [19] presented a sequence of transformation leading to the formation of Ti based on thermogravimetric analysis. The theory developed involves a two-step transformation from $TiH_2 > TiH_x > Ti$. In the present work, the chemical nature of the final metallic layer was confirmed as being elemental Ti by X-ray diffraction. As shown in Fig. 6, the XRD pattern of the activated ceramic foam shows peaks not present in the base alumina which were identified as elemental Ti. The other characteristic Ti peaks which are apparently not present overlap with those of the alumina and are thus simply hidden. Lee et al. [20] obtained similar patterns for the dehydrogenation of TiH_2 to elemental Ti. While the localized presence of other Ti phases cannot be completely excluded, the reduction process was considered as having achieved the goal of obtaining elemental Ti coverage.

In contrast to the uniform macroscopic appearance of the Ti coating, microscopic analysis showed the Ti particle coating after reduction to consist of isolated areas, or spots, of activator randomly distributed over the foam surface (Fig. 7). As

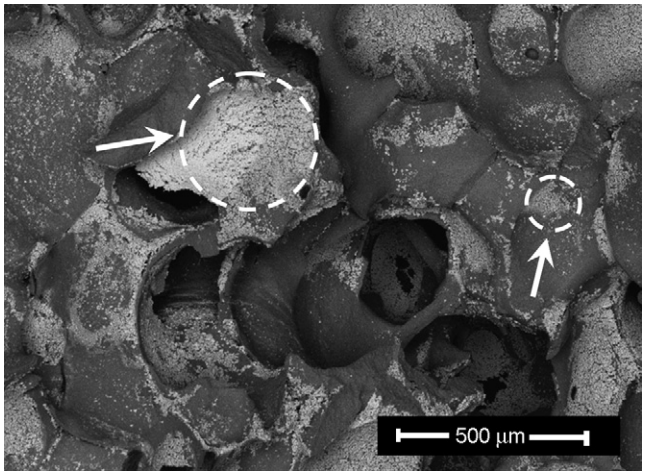

Fig. 7. "Spots" of Ti particles covering the ceramic foam surface after reduction (light grey areas, exemplary marked by dotted circles and white arrows).

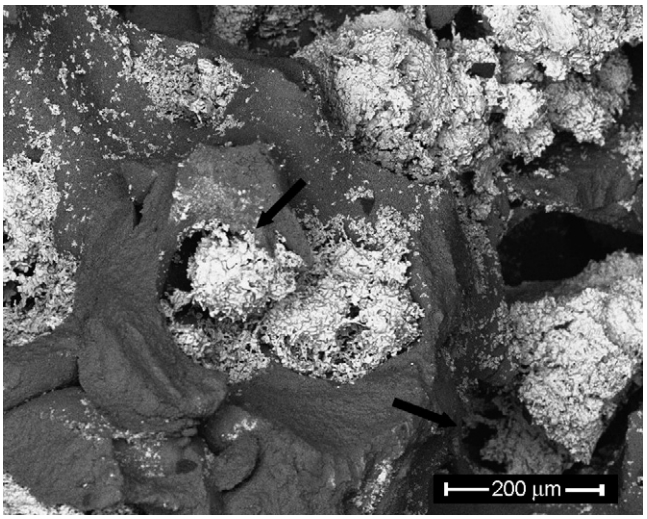

Fig. 8. Alumina foam channels blocked by aggregates of Ti particles (black arrows).

mentioned previously, higher concentrations of Ti particles could be found near the foam sample surfaces, and here channels completely blocked by Ti particles were observed (Fig. 8).

Despite these heterogeneities in the distribution of the activator, subsequent steel infiltration was achieved in the activated zones. The metal matrix was intimately connected to the ceramic network and no gap could be detected at the interfaces between the ceramic and the metal.

SEM investigations did reveal some Ti-rich areas mixed with inclusions of alumina particles in the metal matrix (Fig. 9). Quantitative analysis by EPMA of the Ti-rich areas clearly showed large amounts of Ti and O (48 and 37 at.%, respectively). C and N were also detected, but at lower concentrations (3 and 6 at.%, respectively). The dominance of O over C and N implied that TiO_x is the main constituent of this phase. Around these Ti-rich areas, the metal matrix developed in a needle-like structure which is characteristic for the eutectic microstructure in steel. Here, the EPMA analysis revealed a high Ti content. In comparison with standard steel, the Ti

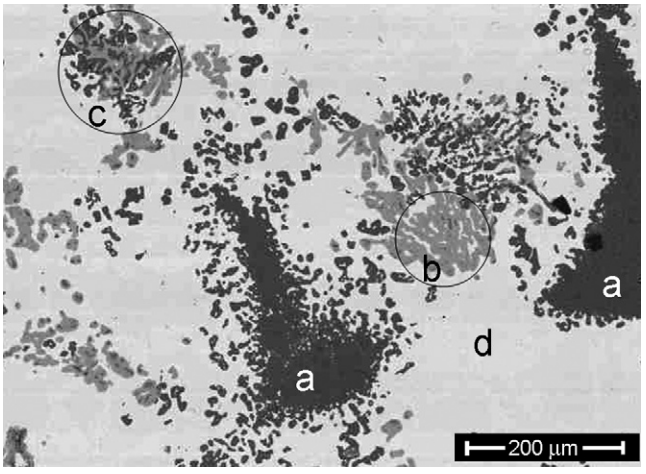

Fig. 9. TiH_2 activated alumina foam after infiltration with steel X38CrMoV5-1. (a) Ceramic struts, (b) Ti-rich areas, (c) Ti-rich area mixed with free alumina particles and (d) steel.

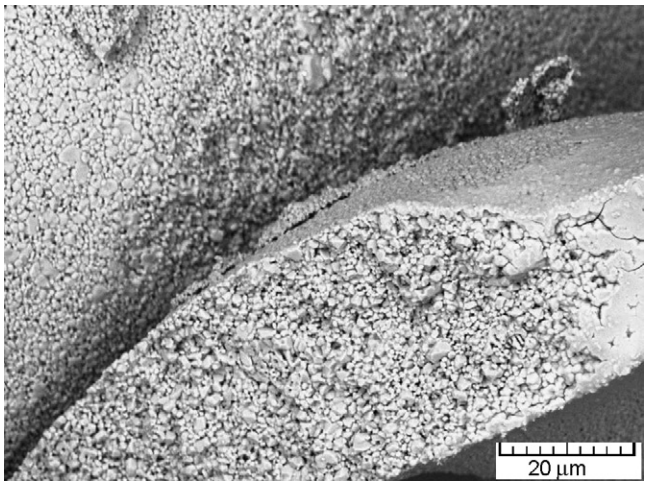

Fig. 10. Fracture surface of a strut in a sintered alumina foam (90 ppi).

content increases to ∼13 at.% of the complete composition, whereas the Fe-content drops to 70 at.% (instead of ∼90 at.%). The resulting Ti/Fe ratio corresponds to that at the eutectic point of the Ti–Fe phase diagram (16 at.% Ti/84 at.% Fe) and therefore correlates well with the eutectic microstructure observed with the SEM.

In the Ti-rich areas with alumina inclusions (e.g. Fig. 9c), the alumina inclusions are loosely arranged in a geometrical form reminiscent of the cross-section of a strut. Therefore, although the inner part of some struts are apparently dense (e.g. Fig. 9a), the metal matrix could infiltrate the open porosity of these structures. An explanation for this might be that the Ti-rich molten steel is highly corrosive and creates thermochemical reactions at the alumina surfaces which lead to the creation of inclusions of alumina particles which are only loosely bonded to the strut. Alternatively, it is possible that the metal melt intruded into porosity in these struts which was present after sintering of the alumina foam. In fragments of sintered foams analysed with the SEM, sintering necks between individual alumina particles seemed to be almost non-existent in some struts (Fig. 10), indicating that the densification process of the alumina had not been completed during the sintering cycle and resulting in a highly porous structure. Work to optimize the alumina microstructure by modifying the sintering cycle (dwell time and dwell temperature) is continuing.

4. Conclusions

Metal matrix composites with three-dimensional interconnected ceramic/metal structures have been successfully produced. The initial alumina foams with between 20 and 90 ppi were successfully activated by two different routes involving either application of a halide salt or of TiH_2.

With the halide salt route, activation was achieved only with large pore size alumina foams (20 and 30 ppi). A uniform Ti particle layer with a thickness of ∼10 μm could be applied to the ceramic with this process. With smaller pores (80 ppi), the activation front did not reach the center of the foam blocks. This finding was attributed to blocking of the fine pore channels with the relatively coarse salt powder. The activation level of the 20 and 30 ppi foams was sufficient to enable the infiltration with Ni-base alloy Inconel 625, however, the velocity of the infiltration front appears to have been too high because large pores were only partially filled with the metal. Closer analysis of large pores also revealed unsatisfying interfaces between the foam and the metal, with up to 10 μm gaps between the two being found in some cases. The difference in the thermal expansion coefficients of the two materials may be responsible for the appearance of such gaps.

Foams with smaller pore size (90 ppi) could be activated via the TiH_2 route. Microscopically, spots of the activator were distributed all over the ceramic foam surface. In close proximity of the external sample surface, a filter effect led to the blocking of ceramic foam channels with TiH_2. Despite this, the activated blocks of ceramic foam were easily infiltrated with steel, making the fabrication of a three-dimensional MMC possible. Excess Ti locally modified the steel matrix composition which induced the formation of microstructural singularities in the matrix of the infiltrated MMC. In some cases Ti-rich areas mixed with alumina particles could be observed.

5. Outlook

These basic experiments with alumina foams have convincingly demonstrated that it is possible to activate and infiltrate foams with pores with an average diameter of ∼280 μm. In general, however, the MMCs exhibit only low ceramic volume fractions in the range of ∼20 vol.% and the struts of the foams are usually narrow compared to the width of pore channels. Equal proportions of metal and ceramic in uniform distribution would be ideal, and work will be carried out in this area to achieve MMCs exhibiting such microstructures.

Acknowledgements

The authors wish to thank A. Broenstrup for assisting with the preparation of the ceramic foams, and B. Zigerlig for the binder preparation and the discussions regarding the experimental set-up for the TiH_2 activation route. M. Wegmann is gratefully acknowledged for the helpful comments.

References

[1] S. Skirl, R. Krause, S.M. Wiederhorn, J. Roedel, Processing and mechanical properties of Al_2O_3/Ni_3Al composites with interpenetrating network microstructure, J. Am. Ceram. Soc. 84 (2001) 2034–2040.
[2] H. Prielipp, M. Knechtel, N. Claussen, S.K. Streiffer, H. Muellejans, M. Ruehle, J. Roedel, Strength and fracture toughness of aluminum/alumina composites with interpenetrating networks, Mater. Sci. Eng. A 197 (1995) 19–30.
[3] L.S. Sigl, P.A. Mataga, B.J. Dalgleish, R.M. McMeeking, A.G. Evans, On the toughness of brittle materials reinforced with a ductile phase, Acta Metall. 36 (4) (1988) 945–953.
[4] T. Clyne, P. Withers, An Introduction to Metal Matrix Composites, first ed., Cambridge Press, Cambridge, 1995.
[5] A. Mattern, B. Huchler, D. Staudenecker, R. Oberacker, A. Nagel, M.J. Hoffmann, Preparation of interpenetrating ceramic–metal composites, J. Eur. Ceram. Soc. 24 (2004) 3399–3408.

[6] F. Lange, V. Bhasckar Velamakanni, A. Evans, Method for processing metal-reinforced ceramic composites, J. Am. Ceram. Soc. 73 (2) (1990) 388–393.
[7] C. Toy, W.D. Scott, Ceramic–metal composite produced by melt infiltration, J. Am. Ceram. Soc. 73 (1) (1990) 97–101.
[8] E. Lugscheider, W. Tillmann, W. Weise, Entwicklung von hochtemperaturbeständigen aktivlötverbindungen aus nichtoxidkeramik, Metallurgy 48 (1994) 27–33.
[9] J.G. Li, Wetting of ceramic materials by liquid silicon, aluminium and metallic melts containing titanium and other reactive elements: a review, Ceram. Int. 20 (1994) 391–412.
[10] Yu.V. Naidich, V.S. Zhuravlev, V.G. Chuprina, Adhesion, wetting, and formation of intermediate phases in systems composed of a titanium-containing melt and an oxide II. Systems Ni–Ti/Al_2O_3 and Ni–Mo/ Al_2O_3, Poroshkovaya Metallurgiya 3 (1974) 82–85.
[11] K. Lemster, T. Graule, J. Kuebler, Processing and microstructure of metal matrix composites prepared by pressureless Ti-activated infiltration using Fe-base and Ni-base alloys, Mater. Sci. Eng. A 393 (2005) 229–238.
[12] G. Krauss, J. Kuebler, E. Trentini, Preparation and properties of pressureless infiltrated SiC and AlN particulate reinforced metal ceramic composites based on bronze and iron alloys, Mater. Sci. Eng. A 337 (2002) 233–263.
[13] K. Lemster, T. Graule, T. Minghetti, C. Schelle, J. Kuebler, Short overview of mechanical and machining properties of X38CrMoV5-1/Al_2O_3 metal matrix composites and components, Mater. Sci. Eng. A 420 (2006) 296–305.
[14] H.W. Lavendel, Metalized-ceramic/metal composites, Ceram. Bull. 53 (1974) 797–808.
[15] E. Breval, J. Cheng, D.K. Agrawal, Development of titanium coatings on particulate diamond, J. Am. Ceram. Soc. 83 (2000) 2106–2108.
[16] K. Schwartzwalder, H. Somers, A. Somers, Method of making porous ceramic articles, US Patent No. 3,090,094 (1963).
[17] J. Saggio-Woyansky, C.E. Scott, Processing of porous ceramics, Am. Ceram. Soc. Bull. 71 (1992) 1674–1682.
[18] H. Elsener, U. Koltz, F.A. Khalid, D. Piazza, M. Kiser, The role of binder on microstructure and properties of a Cu-base active brazing filler metal for diamond and cBN, Adv. Eng. Mater. 7 (5) (2005) 375–380.
[19] V. Bhosle, E.G. Baburaj, M. Miranova, K. Salama, Dehydrogenation of nanocrystalline TiH_2 and consequent consolidation to form dense Ti, Metall. Mater. Trans. A 34A (2003) 2793–2799.
[20] W. Lee, S. Hyunho, W.Y. Lee, Microstructural evolution during the hot-pressing of TiH_2–TiC particle mixtures, Scripta Mater. 48 (2003) 719–724.